DOI. 10.1109/CINTI-MACRo57952.2022.10029500

Evaluation of the Use of an Intelligent System in the Calibration of a Refined Car-Following Model

Mădălin-Dorin Pop
Computer and Information Technology Department
Politehnica University of Timişoara
Timişoara, România
madalin.pop@upt.ro

Octavian Proştean
Automation and Applied Informatics Department
Politehnica University of Timişoara
Timişoara, România
octavian.prostean@upt.ro

Mihai V. Micea
Computer and Information Technology Department
Politehnica University of Timişoara
Timişoara, România
mihai.micea@cs.upt.ro

***Abstract*—This paper aims to extract the computational logic of a hybrid method for online calibration of car-following models and apply it to a refined car-following model that incorporates the behavior of vehicles moving on the adjacent traffic lanes. This calibration method combines the concept of Kalman filters with the Takagi–Sugeno Fuzzy Inference System (T-S FIS). Furthermore, this paper analyzes the influence of the lane change behavior on the calibration process. The testing of the hybrid calibration method in the case of a refined car-following model uses real traffic data and it is followed by a discussion of the results based on day/night traffic behaviors.**

Keywords—computational intelligent system, fuzzy inference, refined car-following model, Takagi-Sugeno, Kalman filter, online calibration, lane change behavior

I. INTRODUCTION

Recent developments in road traffic management focus on intelligent transportation systems (ITS). The need for these approaches arises as a consequence of the extension of road infrastructures and the increase of traffic congestion, especially in urban areas.

Many solutions for traffic management use microscopic traffic models. Data used by these models consist of characteristics such as vehicle speed, acceleration, running distance between the vehicles moving in a chain through a traffic lane. All these data can be easily retrieved in real-time using sensor networks specific to traffic monitoring such as inductive loops, infrared sensors, video cameras, etc. The modeling process aims to provide a simulated model closer to the real model observed. This model can be further used to predict the future evolution of traffic characteristics which has a high impact on crossroads management (e.g., green-intervals settings, decision-making process regarding the adoption of an appropriate type of crossroad configuration – roundabout, traffic lights, etc.). Furthermore, the acquisition of traffic data can influence the modeled system through errors introduced during the measurement of traffic characteristics. According to these assumptions, there arises the need for high-accuracy traffic models.

The calibration process involves a continuous validation of the parameters of the simulated model through a comparison with the traffic characteristics in real-time of the observed model. The output of this process consists of the identification of the compensation values, further called offsets, that should be applied to the simulated model until it faithfully reproduces the observed model.

The purpose of this paper is to adapt the calibration method proposed by Pop et al. [1] to the needs of the refined car-following model [2-4]. In addition to previous studies, this paper provides testing and analysis of the performance of the proposed calibration method for both daytime and nighttime traffic behaviors.

II. RELATED WORK

The calibration of car-following models is challenging and depends on the correctness of selected measures of performance and goodness-of-fit functions [5]. Punzo et al. [5] conducted a research on the calibration of car-following models designed for both human and automated-driven vehicles. They provided a guideline for the calibration of these models and discouraged "*the use of the objective functions which have consistently shown to be either not Pareto-efficient, or not preferable according to the proposed criterion across all the models and datasets*" [5].

The root mean squared error (RMSE) is the metric chosen in several studies to characterize the goodness of fit of the chosen calibration method. Gunter et al. [6] provide a comparison between three well-known car-following models (i.e., optimal velocity with relative velocity model – OVRV, intelligent driver model – IDM, and Gazis-Herman-Rothery model – GHR) in the context of automated-driven vehicles. They concluded that OVRM and IDM behave better than GHR in the context considered. Shang and Stern [7] compared the calibration results for OVRM, optimal velocity-follow the leader (OV-FTL), and IDM considering human-driven vehicles. The experimental results showed that the simulated IDM does not reproduce the real traffic as well as OVRM and OV-FTL under the same noise.

Several papers present calibration methods based on artificial intelligence concepts. Nguyen and Stern [8] used RMSE to analyze the calibration of a new car-following model that uses reinforcement learning to address the oscillatory conditions of real traffic in the case of human-driven vehicles. A comparison with IDM showed satisfactory results of the proposed model, especially in the case of low-speed oscillatory driving conditions. Abodo et al. [9] combined the concepts of Bayesian inference and probabilistic programming in IDM calibration.

Pourabdollah et al. [10] proposed a method that combines the application of the goodness-of-fit function with the use of three measures of performance. This approach was tested and validated by calibrating the following models: IDM, Krauss, and Wiedemann. This method showed significant improvements in the case of IDM, but for Krauss and Wiedemann, larger errors compared to IDM were still reported.

III. MICROSCOPIC TRAFFIC MODELING

In addition to mesoscopic and macroscopic traffic modeling concepts, microscopic traffic modeling provides a

more detailed overview of road traffic phenomena. Yin et al. [11] described the dynamic microscopic traffic model as a system containing the following levels of representation: crossroads configuration, links, lane choice behavior, and car-following. The last two levels have a great impact on describing the interactions between vehicles moving in parallel traffic lanes, in the same direction.

At this microscopic level of modeling, the accuracy of vehicle motion parameters (e.g., acceleration, velocity, running distance), also called dynamic characteristics, is crucial for traffic collision avoidance. Fig. 1 illustrates the components of a control system for microscopic traffic. Real-time data, which characterize the observed model, represent the input for both the modeled system and the validation system. Based on previous data from time $t-\tau$, the modeled traffic system predicts the parameters' values from time t. The simulation processes these values and forwards them to the validation system responsible for a comparison with the real-time data retrieved at time t. The result of this validation represents the estimation error that is further processed by the calibration system that establishes the offsets to be applied to the modeled system. This process ends when the estimation errors identified during validation are equal to zero, with the modeled system being calibrated.

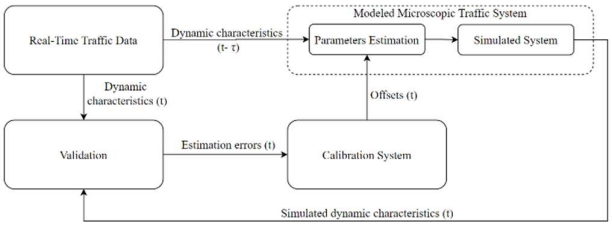

Fig. 1. Control system for microscopic traffic – general overview.

A. Car-following Concept

As a level of the road network load model, the car-following model describes the dynamic interaction between vehicles moving in a chain on a traffic lane considering pairs of two vehicles (Fig. 2). The vehicle ahead represents the leader vehicle (LV), and the vehicle behind is called the follower vehicle (FV). The FV should dynamically adapt the acceleration control strategy based on the behavioral driving changes of the LV to avoid collisions. In Fig. 2, x_2 and x_4 represent the running distances of LV and FV, $s(t-\tau)$ and $s(t)$ represent the dynamic distances between LV and FV at time $t-\tau$ and t, respectively.

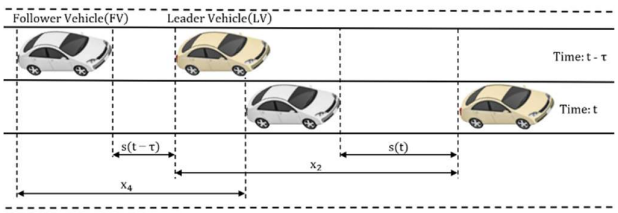

Fig. 2. Car-following model – dynamic characteristics.

Equation (1) describes the state-space representation of the car-following model in continuous time and without time delay [12-13]. In addition to the previously described notations for vehicle characteristics, x_1 and x_3 represent the velocities of LV and FV, u_1 and u_2 are the accelerations of LV and FV, and S represents the standard safety distance responsible for collision avoidance which depends on the vehicle length L.

$$\begin{cases} \begin{bmatrix} \dot{x}_1 \\ \dot{x}_2 \\ \dot{x}_3 \\ \dot{x}_4 \end{bmatrix} = \begin{bmatrix} 0 & 0 & 0 & 0 \\ 1 & 0 & 0 & 0 \\ 0 & 0 & 0 & 0 \\ 0 & 0 & 1 & 0 \end{bmatrix} \cdot \begin{bmatrix} x_1 \\ x_2 \\ x_3 \\ x_4 \end{bmatrix} + \begin{bmatrix} 1 & 0 \\ 0 & 0 \\ 0 & 1 \\ 0 & 0 \end{bmatrix} \cdot \begin{bmatrix} u_1 \\ u_2 \end{bmatrix} \\ y = \begin{bmatrix} 0 & -1 & 0 & 1 \end{bmatrix} \cdot \begin{bmatrix} x_1 \\ x_2 \\ x_3 \\ x_4 \end{bmatrix} + \underbrace{L \cdot \left(1 + \frac{x_3}{16.10}\right)}_{S} \end{cases} \quad (1)$$

Taking into account the notations from (2), the state-space representation from (1) can be rewritten according to (3) [12-13]:

$$\begin{aligned} \bar{x}_1 &= x_3 - x_1 \\ \bar{x}_2 &= x_4 - x_2 = s \\ \bar{y} &= \bar{x}_2 \end{aligned} \quad (2)$$

$$\begin{cases} \begin{bmatrix} \dot{\bar{x}}_1 \\ \dot{\bar{x}}_2 \end{bmatrix} = \begin{bmatrix} 0 & 0 \\ 1 & 0 \end{bmatrix} \cdot \begin{bmatrix} \bar{x}_1 \\ \bar{x}_2 \end{bmatrix} + \begin{bmatrix} -1 & 1 \\ 0 & 0 \end{bmatrix} \cdot \begin{bmatrix} u_1 \\ u_2 \end{bmatrix} \\ \bar{y} = \begin{bmatrix} 0 & 0 \\ 0 & 1 \end{bmatrix} \cdot \begin{bmatrix} \bar{x}_1 \\ \bar{x}_2 \end{bmatrix} \end{cases} \quad (3)$$

Based on previous assumptions, the traditional multiple input multiple output (MIMO) state-space representation from (4) for the continuous-time car-following model described by (1) has the matrices $[A \quad B]$ are controllable and $[A \quad C]$ observable [12-13]. In addition, the system has the eigenvalues equal to zero.

$$\begin{cases} \dot{\bar{x}}(t) = A \cdot \bar{x}(t) + B \cdot u(t) \\ \bar{y}(t) = C \cdot \bar{x}(t) + S \end{cases} \quad (4)$$

B. Lane Change Behavior

Lane change consists of an action taken by a driver to initiate the movement to join another adjacent traffic lane. This action contains a degree of uncertainty regarding the driver behavior, but some of them can be predicted (e.g., lane change initiated to a traffic lane that allows the drive to leave the road network, lane change because of low velocity in the movement of LV, etc.). The last situation enables the FV to become the new LV, in the case of a return to the initial traffic lane. Besides this possible switch in vehicle role, the movement to an adjacent traffic lane implies the integration of the vehicle initiating the maneuver as the new FV for the vehicle ahead and the new LV for the vehicle behind in the movement chain.

Taking into account that L_{i-1}, L_i, and L_{i+1} are the right, middle, and left traffic lanes, Fig. 3 illustrates a lane change action of the FV_{L_i} from L_i to L_{i+1}. Each traffic lane is modeled using the single-lane approach for car-following models. After this action the old FV_{L_i} from L_i becomes the new $FV^*_{L_{i+1}}$ ("*" emphasizes the new role) from L_{i+1}. In this

way, $FV^{*}_{L_{i+1}}$ should adjust the acceleration control strategy according to the behavior of $LV_{L_{i+1}}$. Furthermore, this action also affects the old $FV_{L_{i+1}}$ movement, being necessary to adapt its dynamic characteristics to the new leader ($FV^{*}_{L_{i+1}}$). At any time, the $FV^{*}_{L_{i+1}}$ can return to its initial traffic lane L_i.

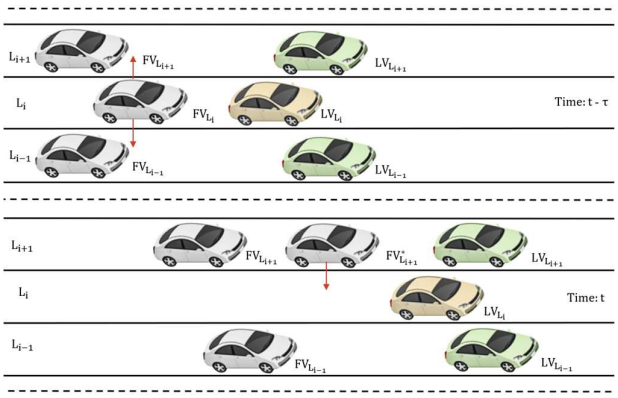

Fig. 3. Lane change action from traffic lane L_i to L_{i+1} [2-3].

C. Online Calibration of Car-Following Models

The need for calibration of car-following models arises from possible existing errors in the measurement of traffic characteristics, or during the parameter estimation in the case of the traffic modeling process. The purpose of an online calibration system is to cover these erroneous values by applying compensation values (offsets) to the modeled system inputs to reduce the difference compared to the real observed system based on a real-time validation with the parameters retrieved from the last one.

Kalman filters have proved their efficiency in the online calibration of microscopic traffic models. Shi et al. [14] argued that even if the Kalman filtering concept usually applies in the calibration of state-space models in discrete-time, it is also appropriate for state-space models in continuous-time. Equation (5) describes the state equations adapted to the needs of the car-following model as defined by Punzo et al. [15]. The notation $\gamma_i, i = \{1, 3, s\}$ describes the model parameters that need calibration and T is the space length.

$$\begin{cases} \dot{x}_1(t) = x_1(t) + \gamma_1(t) \\ \dot{x}_3(t) = x_3(t) + \gamma_3(t) \\ \dot{s}(t) = s(t) + \left[x_1(t) - x_3(t)\right] \cdot T + \gamma_s(t) \end{cases} \tag{5}$$

The output of the calibration system defined in (6) [15] depends on the measurement errors $\zeta_i, i = \{1, 3, s\}$ of the traffic parameters as follows:

$$\begin{cases} \dot{x}_1^{obs}(t) = x_1(t) + \zeta_1(t) \\ \dot{x}_3^{obs}(t) = x_3(t) + \zeta_3(t) \\ \dot{s}^{obs}(t) = s(t) + \zeta_s(t) \end{cases} \tag{6}$$

The state-space representation for the Kalman filter becomes as follows [15]:

$$\begin{cases} \dot{x}(t) = A_k \cdot x(t) + B_k \cdot u(t) + \gamma(t) \\ y(t) = C_k \cdot x(t) + \zeta(t) \end{cases} \tag{7}$$

where $A_k = \begin{bmatrix} 1 & 0 & 0 \\ 0 & 1 & 0 \\ T & -T & 1 \end{bmatrix}$, $B_k = [0]$ and $C_k = D_k = \begin{bmatrix} 1 & 0 & 0 \\ 0 & 1 & 0 \\ 0 & 0 & 1 \end{bmatrix}$.

The estimated values of the Kalman filter $\hat{x}(t)$ defined in (8) [15] consider the gain matrix K_k and the prediction $\hat{x}_{pr}(t)$ from previous knowledge computed according to (9) [15] based on the values A_k and B_k of the matrices $A_{k_{t-1}}$ and $B_{k_{t-1}}$ at time $t - 1$.

$$\hat{x}(t) = \hat{x}_{pr}(t) + K_k \cdot \left[\gamma(t) - C_k \cdot \hat{x}_{pr}(t)\right] \tag{8}$$

$$\dot{\hat{x}}_{pr}(t) = A_{k_{t-1}} \cdot \hat{x}_{pr}(t) + B_{k_{t-1}} \cdot \hat{x}_{pr}(t) \tag{9}$$

Pop et al. [1] proposed a hybrid calibration method (Fig. 4) that uses the approach of Punzo et al. [15] to eliminate the noises by applying Kalman filters to the inputs of the car-following system and introduced a T-S FIS to learn the compensation value patterns. In this way, the model is faster calibrated. Even if T-S FIS are designed for nonlinear systems or systems with time delay, Lam [16] argued that T-S FIS is also applicable for systems in continuous-time.

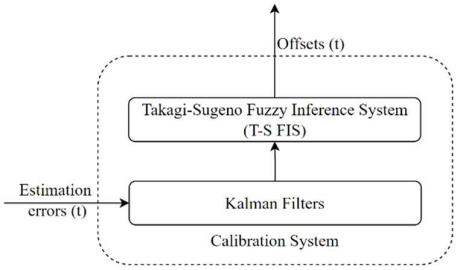

Fig. 4. Hybrid online calibration system based on Kalman filters and T-S FIS [2-3].

Equation (10) defines the fuzzy specific IF-THEN rules of a T-S FIS for a continuous-time model as follows [17-18]:

$$\text{IF } z_1(t) \text{ is } F_{i1} \text{ AND } \ldots \text{ AND IF } z_p(t) \text{ is } F_{ip}$$
$$\text{THEN } \begin{cases} \dot{x}(t) = (A_i + \Delta A_i) \cdot x(t) + (B_i + \Delta B_i) \cdot u(t) \\ y(t) = (C_i + \Delta C_i) \cdot x(t) \end{cases} \tag{10}$$

where $z_j(t), j = \{1, 2, \ldots, p\}$ represent the premise variables, $F_{ij}(t)$ with $i = \{1, 2, \ldots, r\}$ and $j = \{1, 2, \ldots, p\}$ are the fuzzy sets defined for r fuzzy rules, $x(t) \in \mathbb{R}^n$ - the state vector, $u(t) \in \mathbb{R}^m$ - the input vector, $A_i \in \mathbb{R}^{n \times n}$ - the state matrix, $B_i \in \mathbb{R}^{n \times m}$ - the input matrix, $C_i \in \mathbb{R}^{q \times n}$ - the output matrix containing q output parameters, and ΔA_i, ΔB_i, and ΔC_i - the matrices incorporating the uncertainties.

The inferred model takes into account the fuzzy rules from (10) and has the definition from (11) [17-18] where $h_i(z(t))$

represents the normalized grade of membership for each of the i fuzzy rules.

$$\begin{cases} \dot{x}(t)=\sum_{i=1}^{r} h_i\left(z(t)\right)\cdot\left[\left(A_i+\Delta A_i\right)\cdot x(t)+\left(B_i+\Delta B_i\right)\cdot u(t)\right] \\ y(t)=\sum_{i=1}^{r} h_i\left(z(t)\right)\cdot\left(C_i+\Delta C_i\right)\cdot x(t) \end{cases} \quad (11)$$

The normalized grade of membership for each of the fuzzy rules should comply with (12) [17-18].

$$\begin{cases} \sum_{i=1}^{r} h_i\left(z(t)\right)=1 \\ 0<h_i\left(z(t)\right)<1 \end{cases} \quad (12)$$

IV. Calibration of the Refined Car-Following Model

A. Refined Car-Following Model

The refined car-following model proposed by Pop et al. [2] introduces the lane change behavior of the vehicles moving in the adjacent traffic lanes in the control strategy of the acceleration behavior of FV. In this way, the single-lane orientation of the traditional car-following model is extended to multiple-lane roads for the same direction of movement.

The estimation of lane change behavior considers the following factors of influence in driver decision [2, 4]:

- the traffic lane e_{FV} used by the target vehicle to enter the road network;
- the traffic lane d_{FV} used by the target vehicle to leave the road network, also called destination lane;
- the probability of changes in the FV velocity v_{FV} as a feedback to the LV movement behavior.

The first step is to estimate the probability $\hat{P}_{L_j}$ of a lane change action from lane i to j as follows [2]:

$$\hat{P}_{L_j}=\frac{p\left(e_{FV_i}\right)\cdot p\left(d_{FV_i}\right)\cdot p\left(v_{FV_i}\right)}{p\left(L_i\right)}\cdot p_{L_{i\to j}},\ j=\{i\pm 1\} \quad (13)$$

where $p_{L_{i\to j}}$ is the total advantage of the two immediately affected neighboring vehicles computed according to Bayesian rules for conditional probabilities according to (14) [2]:

$$p_{L_{i\to j}}=P\left(d_{FV_j}|L_i\right)\cdot P\left(v_{FV_j}|L_i\right),\ j=\{i\pm 1\} \quad (14)$$

and the lowercase notation represent the probabilities calculated based on previous traffic data as defined by (15) [2].

$$\begin{aligned} p\left(e_{FV_i}\right)&=P\left(L_i|e_{FV_i}\right)\cdot P\left(e_{FV_i}\right) \\ p\left(d_{FV_i}\right)&=P\left(L_i|d_{FV_i}\right)\cdot P\left(d_{FV_i}\right) \\ p\left(v_{FV_i}\right)&=P\left(L_i|v_{FV_i}\right)\cdot P\left(v_{FV_i}\right) \\ p\left(L_i\right)&=P\left(L_i\right)\cdot P\left(L_i\right)\cdot P\left(L_i\right) \end{aligned} \quad (15)$$

To simplify the understanding of the acceleration control strategy it is necessary to define the notations from (16) where $u_{2^2_{L_i}}$ is the acceleration of the successor of FV_{L_i} [19].

$$\begin{cases} u_{driver}=u_{2^*_{L_i}}(t+\tau)-u_{2_{L_i}}(t) \\ u_{newfollower}=u_{2_{L_{i+1}}}(t+\tau)-u_{2_{L_i+1}}(t) \\ u_{oldfollower}=u_{2^2_{L_i}}(t+\tau)-u_{2^2_{L_i}}(t) \end{cases} \quad (16)$$

According to the approach for the refined car-following model, the politeness factor used in the incentive criteria rules for lane change defined by [19] is replaced by the probability $\hat{P}_{L_j}$ of a lane change action from lane i to j from (13) as follows, depending on the type of lane change:

- symmetric lane change [2]:

$$u_{driver}+\hat{P}_{L_j}\cdot\left(u_{newfollower}+u_{oldfollower}\right)>\Delta u_{th},\ j=\{i\pm 1\} \quad (17)$$

- asymmetric lane change (from left to right) [2]:

$$u^{eur}_{FV^*_{L_i}}(t+\tau)-u_{FV_{L_i}}(t)+\hat{P}_{L_j}\cdot u_{oldfollower}>\Delta u_{th}-\Delta u_{bias},\ j=\{i\pm 1\} \quad (18)$$

- asymmetric lane change (from right to left) [2]:

$$u_{FV_{L_i}}(t+\tau)-u^{eur}_{FV^*_{L_i}}(t)+\hat{P}_{L_j}\cdot u_{newfollower}>\Delta u_{th}+\Delta u_{bias},\ j=\{i\pm 1\} \quad (19)$$

where u^{eur}_k, $k=\{FV^*_{L_i}, FV_{L_i}\}$ represent the adjusted accelerations that comply with the legislation of most European countries, Δu_{th} represents the switching threshold and Δu_{bias} is a constant value that describes the keep-right directive of the lane change rule [3, 19].

The refined car-following model assumes that the model updates the dynamic parameters according to (17), (18), and (19) based on the driver's decision c to initiate a lane change maneuver, otherwise, in the absence of a decision the model behaves as a single-lane car-following model. Equation (20) defines the driver decision as the probability of not choosing the lane L_i and is computed based on historical traffic data for a specific road segment [2-3].

$$c=1-P\left(L_i\right) \quad (20)$$

B. Simulation Model

To evaluate the behavior of the T-S FIS calibration system in the case of refined car-following model, a simulation was created in Simulink (MATLAB R2021b). The simulation uses real traffic data for a three-lane road segment located in Calea Șagului (Timișoara, Romania). These data were collected in August 2019 by the local traffic monitoring center through a data acquisition system based on inductive loops. Furthermore, these data were classified in the daytime and nighttime according to the specific civil twilight for the chosen region and period [20].

The simulation (Fig. 5) shows the calculation of the refined acceleration values u1_i_refined and u2_i_refined of the LV and FV moving in the lane L_i, as a switch based on the driver's decision c regarding a lane change action. The calibration system was also highlighted together with a detailed overview of its implementation.

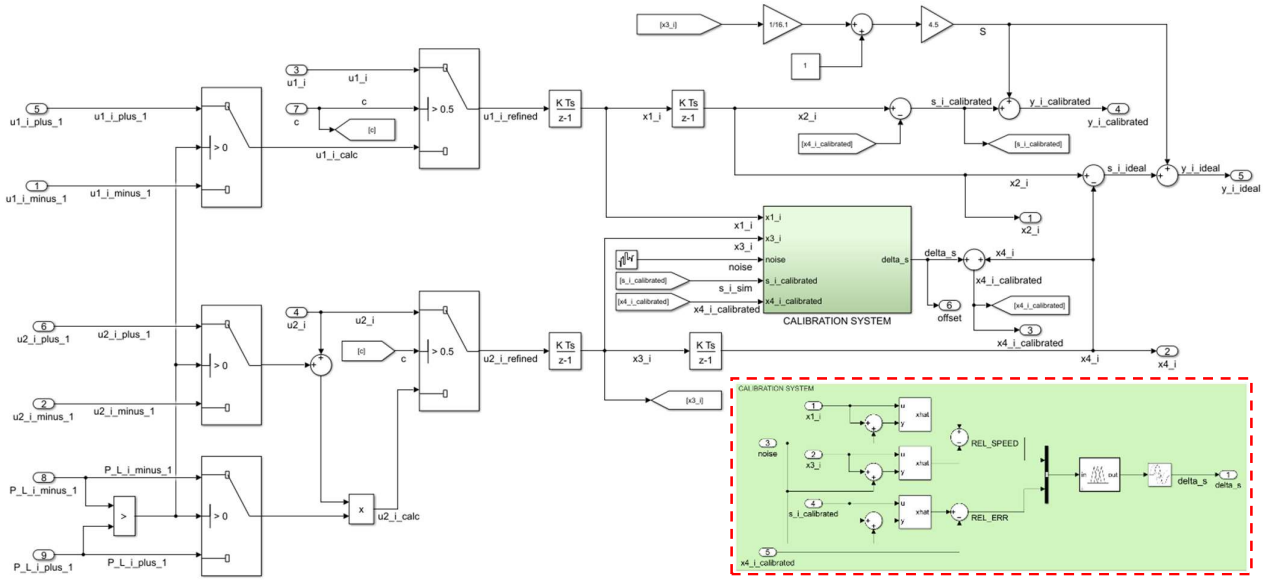

Fig. 5. Simulation model including a detailed overview of the calibration system (located in the right bottom corner of the figure) [1-4].

C. *Evaluation of the Calibration Method*

The following section discusses the calibration of traffic parameters depending on the daytime and nighttime traffic behaviors. The aim of these discussions is to identify specific improvements related to road network loading. Furthermore, this paper also evaluates the performance of the online calibration method based on the mixture between Kalman filters and T-S FIS through a comparison with the Kalman filter-only method for the refined car-following model.

V. Results and Discussions

Figure 6 shows a comparative overview of the simulation results for both daytime and nighttime traffic cases. The running distances and the dynamic safety distances were considered as main data to visualize the calibration results.

For daytime traffic (Fig. 6a) a lane change action is observable at time $t = 6.80$ ms, but at that time, the system being already calibrated, this lane change action does not influence the control of the FV behavior, the calibration status being maintained. Analyzing the behavior for the night traffic (Fig.6b) results that if a lane change action took place before the system was calibrated, this does not influence the calibration process, the system joining the calibrated status after this action. Also, in the case of nighttime traffic a lane change action has been captured at time $t = 3.00$ ms.

The evolution of offset values is similar for both cases. In the case of nighttime traffic, the system is calibrated faster, which is explainable through the reduced traffic during night that leads to lower need for computation resources compared to daytime traffic.

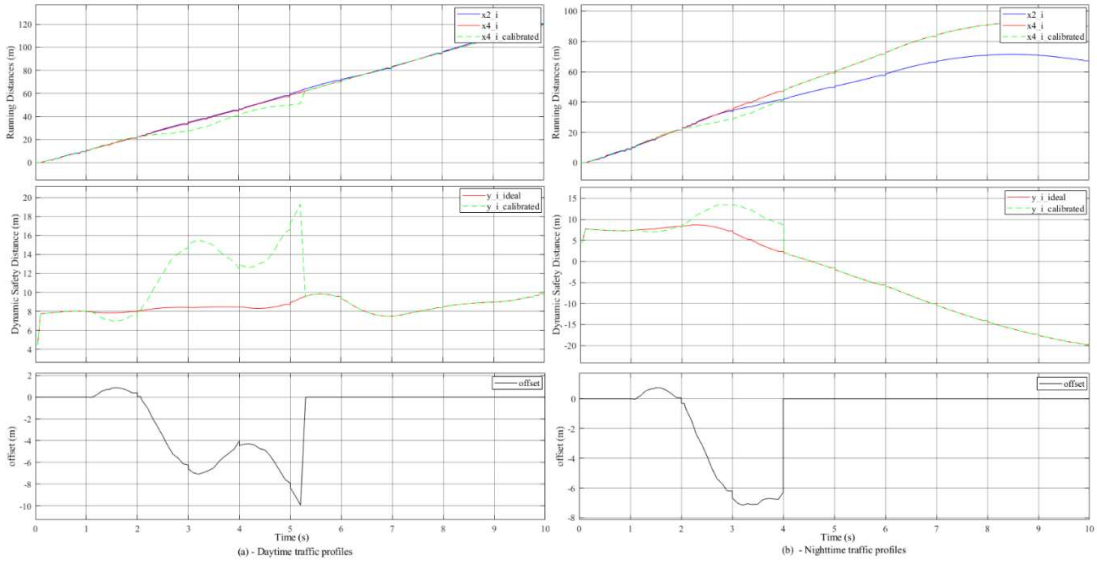

Fig. 6. Simulation results – a comparative overview of (a) - daytime and (b) - nighttime traffic profiles.

The performance overview (Fig. 7) shows that the "*Kalman filter-only approach introduces a uniform increase in computation error that leads to a scaled running distance compared to real traffic conditions*" [1], an error missing in the case of the mixture of Kalman filters with T-S FIS.

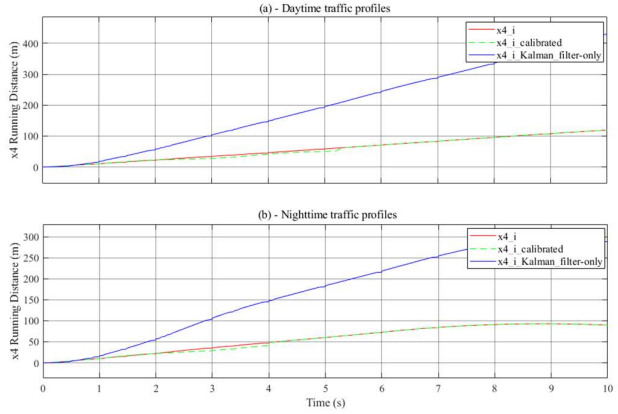

Fig. 7. Performance overview – a comparison between the proposed calibration method and the Kalman filter-only method.

VI. Conclusions

This paper performed an evaluation of the online calibration method based on the mixture between Kalman filters and T-S FIS [1] in the case of a refined car-following model that incorporates the lane change actions of vehicles in adjacent traffic lanes [2-4]. This evaluation shows that the calibration process is delayed in the case of daytime traffic compared to nighttime traffic. This delay is related to the network loading, leading to a short increase in computational processing times propagated from the data acquisition system. The calibration method discussed does not introduce computational delays, fitting to a real-time processing system.

Further research can improve of this calibration method by applying neuro-fuzzy approaches or using macroscopic traffic data as a third linguistic variable for the current T-S FIS.

Acknowledgment

This paper was financially supported by the Project "*Network of excellence in applied research and innovation for doctoral and postdoctoral programs*" / InoHubDoc, project co-funded by the European Social Fund financing agreement no. POCU/993/6/13/153437.

The data used for simulations were received from "*Primăria Municipiului Timişoara - Direcţia Generală Drumuri, Poduri, Parcaje şi Reţele Utilitare - Birou Monitorizare Trafic*", Timişoara, Romania, based on the approved request RE2019-002611/18.12.2019. The support is gratefully acknowledged.

References

[1] M.-D. Pop, O. Proştean, T.-M. David, and G. Proştean, "Hybrid Solution Combining Kalman Filtering with Takagi–Sugeno Fuzzy Inference System for Online Car-Following Model Calibration," *Sensors*, vol. 20, no. 19, p. 5539, Sep. 2020, doi: 10.3390/s20195539.

[2] M.-D. Pop, O. Proştean, and G. Proştean, "Multiple Lane Road Car-Following Model using Bayesian Reasoning for Lane Change Behavior Estimation: A Smart Approach for Smart Mobility," in *Proceedings of the 3rd International Conference on Future Networks and Distributed Systems*, Paris France, Jul. 2019, pp. 1–8. doi: 10.1145/3341325.3341996.

[3] M.-D. Pop, O. Proştean, and G. Proştean, "Fault Detection Based on Parity Equations in Multiple Lane Road Car-Following Models Using Bayesian Lane Change Estimation," *JSAN*, vol. 9, no. 4, p. 52, Nov. 2020, doi: 10.3390/jsan9040052.

[4] M.-D. Pop, "Refined Car-Following Model Incorporating the Behavior of the Vehicles from the Adjacent Lanes," PhD thesis, Politehnica University of Timisoara, Timisoara, 2022. [Online]. Available: https://rei.gov.ro/teza-doctorat-document/83218762a31b52 6b296-22-Teza_Finala_Madalin_13012022_signed.pdf

[5] V. Punzo, Z. Zheng, and M. Montanino, "About calibration of car-following dynamics of automated and human-driven vehicles: Methodology, guidelines and codes," *Transportation Research Part C: Emerging Technologies*, vol. 128, p. 103165, Jul. 2021, doi: 10.1016/j.trc.2021.103165.

[6] G. Gunter, R. Stern, and D. B. Work, "Modeling adaptive cruise control vehicles from experimental data: model comparison," in *2019 IEEE Intelligent Transportation Systems Conference (ITSC)*, Auckland, New Zealand, Oct. 2019, pp. 3049–3054. doi: 10.1109/ITSC.2019.8917347.

[7] M. Shang and R. Stern, "Calibrating heterogeneous car-following models for human drivers in oscillatory traffic conditions," in *2020 Forum on Integrated and Sustainable Transportation Systems (FISTS)*, Delft, South Holland Province, Netherlands, Nov. 2020, pp. 101–106. doi: 10.1109/FISTS46898.2020.9264843.

[8] J. Nguyen and R. Stern, "Modeling oscillatory car following using deep reinforcement learning based car following models," in *2021 7th International Conference on Models and Technologies for Intelligent Transportation Systems (MT-ITS)*, Heraklion, Greece, Jun. 2021, pp. 1–6. doi: 10.1109/MT-ITS49943.2021.9529262.

[9] F. Abodo, A. Berthaume, S. Zitzow-Childs, and L. Bobadilla, "Strengthening the Case for a Bayesian Approach to Car-following Model Calibration and Validation using Probabilistic Programming," in *2019 IEEE Intelligent Transportation Systems Conference (ITSC)*, Auckland, New Zealand, Oct. 2019, pp. 4360–4367. doi: 10.1109/ITSC.2019.8917416.

[10] M. Pourabdollah, E. Bjarkvik, F. Furer, B. Lindenberg, and K. Burgdorf, "Calibration and evaluation of car following models using real-world driving data," in *2017 IEEE 20th International Conference on Intelligent Transportation Systems (ITSC)*, Yokohama, Oct. 2017, pp. 1–6. doi: 10.1109/ITSC.2017.8317836.

[11] B. Yin, M. Dridi, and A. El Moudni, "Adaptive Traffic Signal Control for Multi-intersection Based on Microscopic Model," in *2015 IEEE 27th International Conference on Tools with Artificial Intelligence (ICTAI)*, Vietri sul Mare, Italy, Nov. 2015, pp. 49–55. doi: 10.1109/ICTAI.2015.21.

[12] D. Pan and Y. Zheng, "Optimal control and discrete time-delay model of car following," in *2008 7th World Congress on Intelligent Control and Automation*, Jun. 2008, pp. 5657–5661. doi: 10.1109/WCICA.2008.4593852.

[13] A. Khodayari, R. Kazemi, A. Ghaffari, and N. Manavizadeh, "Modeling and intelligent control design of car following behavior in real traffic flow," in *2010 IEEE Conference on Cybernetics and Intelligent Systems*, Jun. 2010, pp. 261–266. doi: 10.1109/ICCIS.2010.5518546.

[14] P. Shi, El.-K. Boukas, and R. K. Agarwal, "Kalman filtering for continuous-time uncertain systems with Markovian jumping parameters," *IEEE Trans. Automat. Contr.*, vol. 44, no. 8, pp. 1592–1597, Aug. 1999, doi: 10.1109/9.780431.

[15] V. Punzo, D. J. Formisano, and V. Torrieri, "Nonstationary Kalman Filter for Estimation of Accurate and Consistent Car-Following Data," *Transportation Research Record*, vol. 1934, no. 1, pp. 2–12, Jan. 2005, doi: 10.1177/0361198105193400101.

[16] H. K. Lam, "A review on stability analysis of continuous-time fuzzy-model-based control systems: From membership-function-independent to membership-function-dependent analysis," *Engineering Applications of Artificial Intelligence*, vol. 67, pp. 390–408, Jan. 2018, doi: 10.1016/j.engappai.2017.09.007.

[17] R. Abdelkrim, H. Gassara, M. Chaabane, and A. El Hajjaji, "Stability approaches for Takagi-Sugeno systems," in *2015 IEEE International Conference on Fuzzy Systems (FUZZ-IEEE)*, Aug. 2015, pp. 1–6.

[18] A. Bouyahya, Y. Manai, and J. Haggège, "New Lyapunov function for Takagi-Sugeno discrete time uncertain systems," in *2015 7th International Conference on Modelling, Identification and Control (ICMIC)*, Dec. 2015, pp. 1–5. doi: 10.1109/ICMIC.2015.7409347.

[19] A. Kesting, M. Treiber, and D. Helbing, "General Lane-Changing Model MOBIL for Car-Following Models," *Transportation Research Record*, vol. 1999, no. 1, pp. 86–94, Jan. 2007, doi: 10.3141/1999-10.

[20] "Sunrise and sunset times in Timişoara, August 2019." https://www.timeanddate.com/sun/romania/timisoara?month=8&year=2019 (accessed Aug. 20, 2022).